# Characteristics Analysis of Large High Speed Induction Motors Using 3-D Finite Element Method

Katsumi Yamazaki and Satoshi Kuramochi
Chiba Institute of Technology
2-17-1, Tsudanuma, Narashino, Chiba 275-0016, Japan, yamazaki. katsumi@it-chiba.ac.jp

Noriaki Fukushima, Shinichiro Yamada, and Shin Tada
Toshiba Mitsubishi-Electric Industrial Systems Corporation
2-4, Suehiro-cho, Tsurumi-ku, Yokohama, Kanagawa 230-0045, Japan

**Abstract — The characteristics of MW-class high speed induction motors are analyzed by the 3-D finite element methods. First, several approximations are applied to the analysis in order to reduce the computation time without the deterioration of accuracy. Then, the calculated characteristics are compared with the experimental results in order to verify the proposed method. Finally, the loss generation mechanism of the motor is revealed by analyzing the harmonic electro-magnetic fields. It is clarified that the combination of the 2-D and one-rotor-slot 3-D finite element method is suitable for the analysis of the motor. By using this method, the largest harmonic loss component of the motor is specified.**

## I. Introduction

Owing to the progress of computers, finite element methods are widely applied to the characteristics calculation of variable speed motors driven by inverters. However, there are few papers that dealt with the analysis of large induction motors whose output is over 1 MW, because of following reasons:

(a) 3-D analysis is required in order to accurately estimate the secondary current by considering the end effect. Small time steps are also required in order to accurately take into account the inverter carrier.

(b) Long time calculation term is required in order to obtain the steady state characteristics because the time constant of electrical transient phenomenon is very large, whereas the rotor slip is very small in the case of the large motors.

(c) A very large number of 3-D finite elements is required in the analysis because the stator cores of the MW-class motors are divided into dozens of packets for cooling.

As a consequence, the full 3-D time-stepping finite element method is hardly applied to the characteristics calculation.

To overcome these difficulties, we firstly investigate the approximation methods for the analysis of large high speed induction motors driven by inverters in order to reduce the calculation time without the deterioration of accuracy. Then, the calculated characteristics are compared with the experimental results in order to verify the proposed method. Finally, the loss generation mechanism of the motor is revealed by analyzing the harmonic electro-magnetic fields.

## II. Analyzed Motor and Calculation Method

Table I lists the specification of the analyzed motor. Fig. 1 shows the photograph and core structure of the motor.

TABLE I
SPECIFICATION OF ANALYZED MOTOR

| | |
|---|---|
| Phases and poles | 3 phases, 2 poles |
| Rating output | 4 MW |
| Maximum rotational speed | 10000 $min^{-1}$ |
| Slip | 0～0.3% |
| Number of stator/rotor slots | 54 (stator) 46 (rotor) |
| Rotor-cage material | Copper alloy |
| Thickness of electrical steel sheet for stator/rotor core | 0.35 mm (stator)<br>0.5 mm (rotor) |
| DC voltage of inverter | 6 kV |

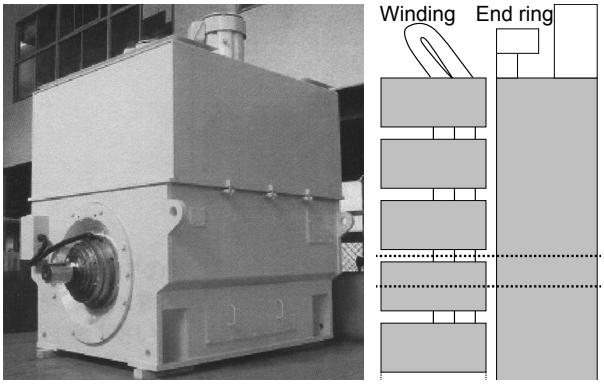


Fig. 1. Photograph and core structure of analyzed motor.

The stator core is divided by the duct spaces for cooling. The motor is driven by a three level PWM inverter using gate communicated turn off thyristors.

First, several approximated methods are applied to the motor. Fig. 2 shows the meshes used in each method.

Fig. 2 (a) is the full 3-D mesh for the motor. The duct spaces are modeled by modifying the permeability of the core in order to reduce the finite elements, as follows:

$$\mu' = \alpha\mu + (1-\alpha)\mu_0 \qquad (1)$$

where $\mu$' and $\mu$ are the modified and original permeability of the core, respectively; $\mu_0$ is the vacuum permeability; $\alpha$ is the ratio of core length to the total motor length including the duct space.

Fig. 2 (b) is the 3-D mesh for half the axial length of one stator-core packet. In this case, the effect of the duct space is exactly considered. On the other hand, the end-effect is neglected. Therefore, the conductivity of the rotor cage is modified by using following expression [1].

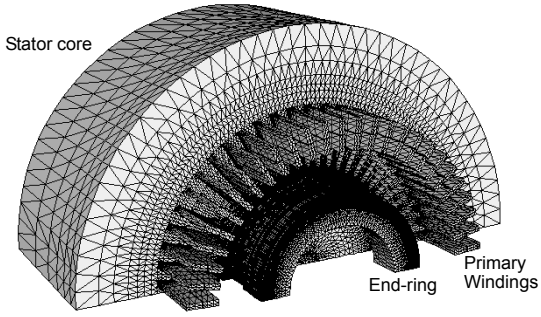


(a) Full 3-D model (1,510,044 tetrahedral edge elements)

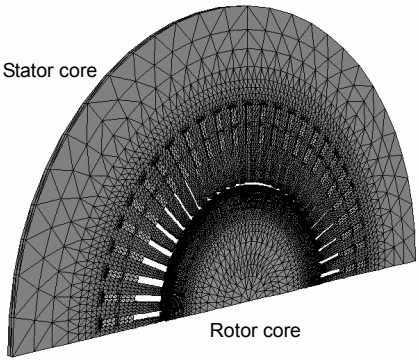


(b) One packet 3-D model (317,904 tetrahedral edge elements)

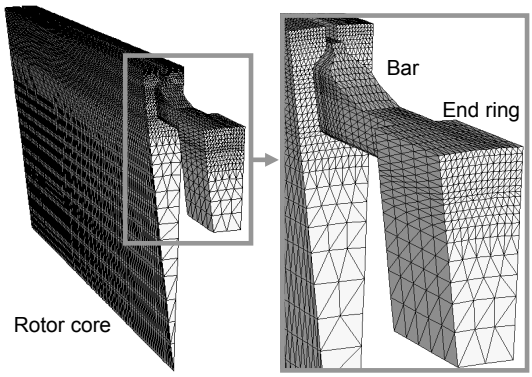


(c) One-rotor-slot 3-D model (367,308 tetrahedral edge elements)

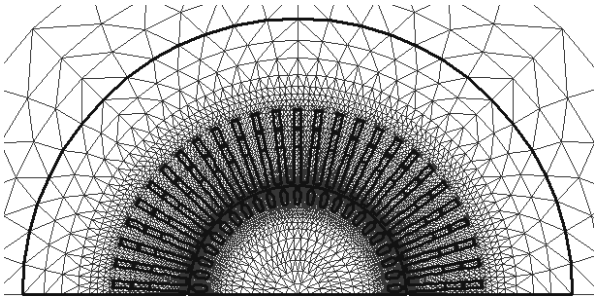

(d) 2-D model (26,492 triangular elements)

Fig. 2. Models for finite element analysis.

$$\sigma' = (1-k)\sigma = \left(1 - \left|\frac{\int_{Sbar}\int_A^B \nabla\phi \cdot dldS}{\int_{Sbar}\int_A^B js\omega \boldsymbol{A} \cdot dldS}\right|\right)\sigma \quad (2)$$

where $\sigma'$ and $\sigma$ are the modified and original conductivity of the rotor cage, respectively; $s\omega$ is the slip angular frequency; $k$ is the ratio of the voltage drop of the end-rings to the total secondary induced voltage; $\boldsymbol{A}$ and $\phi$ are the magnetic vector and electric scalar potentials imposing the gauge condition, as follows:

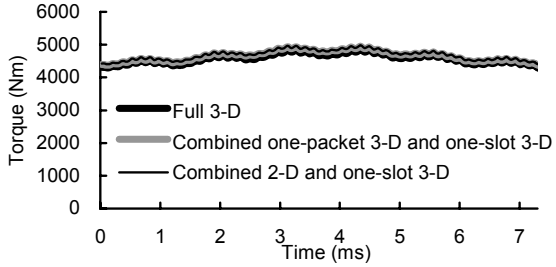


Fig. 3. Calculated torque waveforms (8200 rpm, slip 0.31).

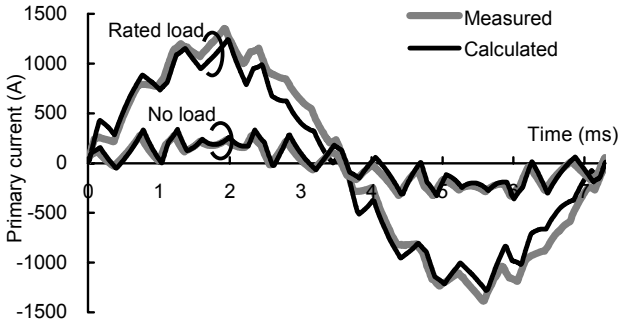


Fig. 4. Measured and calculated primary current waveforms (8200 rpm).

$$A_\theta = 0 \quad (3)$$

where $A_\theta$ is the circumferential component of the magnetic vector potential. By neglecting the variation in $k$ with the harmonic order of secondary currents, the $\boldsymbol{A}$ and $\phi$ can be obtained by the frequency domain analysis using one-rotor-slot model, as shown in Fig. 2 (c).

Fig. 2 (d) is the 2-D mesh. In this case, both (1) and (2) are applied in order to take into account both the duct space and the end-rings.

## III. Results and Discussion

Fig. 3 shows the calculated torque of the motor at the rated load condition by using the above-mentioned methods. The inverter carrier is neglected in this case. It is observed that all the results are nearly identical. These results imply that the approximations (1) and (2) are valid. The calculation time of the full 3-D analysis is 6,758 hours, whereas that of the combined 2-D and one slot 3-D analysis is 2 hours. Therefore, we apply the combined analysis for the characteristics calculation involving the inverter carrier.

Fig. 4 shows the measured and calculated primary current waveforms including the carrier. The results are found to be in good agreement. The calculated torque and loss also agree well with the measurement. More results including the harmonic losses will be shown in the full paper.

## IV. References

[1] K. Yamazaki, "Induction Motor Analysis Considering both Harmonics and End Effects Using Combination of 2D and 3D Finite Element Method," *IEEE Trans. Energy Conversion*, vol.14, no.3, pp.698-703, 1999.